

# Developments and structures of mesopores in alkaline-treated ZSM-5 zeolites

Yousheng Tao · Hirofumi Kanoh ·  
Katsumi Kaneko

© Springer Science + Business Media, LLC 2006

**Abstract** ZSM-5 zeolites with  $\text{SiO}_2/\text{Al}_2\text{O}_3$  molar ratio of 24 were treated in 0.05 M aqueous sodium hydroxide solution at 325 K in different periods. The samples were characterized by means of nitrogen adsorption at 77 K, field emission scanning electron microscopy, X-ray diffractometry, and Fourier transform infrared spectroscopy. Analysis of the experimental results showed that the alkaline treatment periods have influence on the developments and structures of mesopores in the alkaline-treated ZSM-5 zeolites. Alkaline treatment initially develops mesopores mainly from the boundary portion of MFI zeolites to the bulk, while prolonged treatment destroys the mesopores, and an optimum mesoporosity is obtained by the treatment for 1.5 h. On the other hand, crystallinities and short-range order in alkaline treated zeolites have remained virtually unchanged according to the examination from X-ray diffractometry and Fourier transform infrared spectroscopy.

**Keywords** ZSM-5 zeolite · Post-synthesis treatment · Characterization of structure · Adsorption hysteresis · Nitrogen adsorption

## 1 Introduction

Zeolites have gained much attention because of their uniform micropore structures and a range of applications. Their three-dimensional network contains channels and cavities of molecular dimensions (Breck, 1974). The crystalline frameworks and narrow pore size distributions impart these materials with size and shape selectivity for guest molecules. They have been widely studied in catalysis as well as in separation and purification fields (Chen et al., 1988; Ghose et al., 1993; Richter et al., 1999; Pires et al., 2001). However, the major drawback of these zeolites is that the small size of the intricate channels ( $< \sim 0.8$  nm) and cavities (typically  $< 1.5$  nm) in the molecular size range imposes diffusion limitations on the reaction rate as well as a high backpressure on flow systems (Kärger et al., 1992; van Donk et al., 2001; Herrmann et al., 1987; Perez-Ramirez et al., 2003). Much effort has been devoted to the development of new zeolite-type materials with larger pores ( $> 1.5$  nm) (Davis, 2002; Corma, 1997). However, the increase in the average pore size of these materials is very modest and they are still not very effective in reactions with large-sized molecules, for example, for cracking the gas oil fraction of petroleum (Davis, 2002).

Development of zeolites with bimodal pore size distributions of mesopores (pore sizes between 2 nm and 50 nm) and micropores (pore size below 2 nm) is thus of great interest. Since diffusivity is proportional to pore diameter, addition of mesopores to zeolites can

Y. Tao (✉) · H. Kanoh · K. Kaneko  
Department of Chemistry, Faculty of Science,  
Chiba University, Chiba 263-8522, Japan  
e-mail: tao@pchem2.s.chiba-u.ac.jp

increase diffusion coefficients more than two orders of magnitude (Kärger et al., 1992). When one reactant is too big or too hydrophobic to penetrate the zeolite pores, mesoporous zeolites are required. Recently it was proved mesoporous zeolites could achieve high dispersion of a catalytic phase due to the increased external surface (Christensen et al., 2004). In many commercial applications, such as cracking of heavy oil fractions, cumene production, and alkane hydroisomerization, mesopore-added zeolites are receiving considerable attention (Corma, 1997, 2003; van Donk et al., 2003; Hartmann, 2004; Tao et al., 2006). Recently an alternative synthesis route so-called dual templating methods using carbon materials that are removed by oxidation has been reported (Jacobsen et al., 2000; Tao et al., 2003). The strategies of this method is to design zeolites with mesopores using supplementary carbon materials as templates, and such materials are carbon black (Jacobsen et al., 2000), multiwall carbon nanotube (Schmidt et al., 2001), carbon nanofiber (Janssen et al., 2003), carbon mesoporous molecular sieve (Sakthivel et al., 2004; Yang et al., 2004), and carbon aerogels (Tao et al., 2003). While another simple approach to modify zeolites with some mesopores has been known as post-synthesis treatments of zeolites, although it is usually adopted to change the properties connected with the silica/alumina ratio such as cation-exchange capacity and catalytic activity. In the faujasites, mainly zeolite Y, post-synthesis hydrothermal dealumination treatments and other chemical treatments form defect domains 5–50 nm in size, which are attributed to mesopores (Lynch et al., 1987; Patzelova et al., 1987; Cartledge et al., 1989; Choi-Feng et al., 1993; Corma et al., 2002). Previous investigation on dissolution of high silica pentasils (silicalite-1, ZSM-5) with different Al content in 5 M aqueous sodium hydroxide solution showed selective removal of the siliceous species from the zeolite framework due to a relative inertness of tetrahedral aluminum centers towards hydroxide attack (Cizmek et al., 1995; Cizmek et al., 1997). Recent studies on the alkaline treatment of MFI-structured zeolite showed that selective extract of framework Si atoms yields mesopores. Ogura et al. showed alkali treatment by using aqueous sodium hydroxide solution created mesopores without changing the microporous structures and acidity of zeolites, and consequently resulted in an enhanced

catalytic activity for cumene cracking (Ogura et al., 2000, 2001). Groen et al. demonstrated that the role of aluminium as a pore-directing agent in the hierarchical porosity development in MFI zeolites by desilication. An optimal molar Si/Al ratio in the range 25–50 has been suggested for an optimal mesoporosity (Groen et al., 2002, 2003, 2004, 2005a, b, c). We most recently reported, under mild alkaline treatment condition with low concentration of aqueous sodium hydroxide solution, the changes in structural properties depended on the  $\text{SiO}_2/\text{Al}_2\text{O}_3$  molar ratios (Tao et al., in press). Alkaline treatment of low  $\text{SiO}_2/\text{Al}_2\text{O}_3$ , 24, ZSM-5 yielded mesopores with a broad pore size distribution. Alkaline treatment of high  $\text{SiO}_2/\text{Al}_2\text{O}_3$ , 200, ZSM-5 did not show evidence of mesopores by nitrogen adsorption at 77 K and argon adsorption at 87 K.

Since a large variety of potential and existing commercial applications are largely due to the adding of mesopores to conventional zeolites, this paper is attempting to describe the mechanism of the mesopore development of ZSM-5 by the method of post-treatment under mild conditions of 0.05 M aqueous sodium hydroxide solution at 325 K.

## 2 Experimental

### 2.1 Sample preparation

Alkaline treated ZSM-5 zeolites were prepared from parent ZSM-5 zeolites with  $\text{SiO}_2/\text{Al}_2\text{O}_3$  molar ratios of 24 in Na form (HSZ-820NAA, Tosoh Corp.). The parent ZSM-5 zeolites were treated in 0.05 M aqueous sodium hydroxide solutions at 325 K for different periods of time from 0.25 h to 4 h. The solution pH slightly changed from initial 11.9 to final 11.5 (TOA pH METER HM-12P, TOA Electronics Ltd.). The resulting slurry was immediately filtered by suction. The filtered cake was then rinsed with distilled water at 325 K and filtered. It was repeated three times to eliminate silicate materials precipitating during the alkaline treatment. Finally the samples were dried in an oven at 383 K overnight. The samples are denoted as e.g. ZSM-5[1 h] with suffix in brackets referring to the alkaline treatment periods, while the parent zeolites are designed as ZSM-5[p].

## 2.2 Characterizations

### 2.2.1 Adsorption

The nitrogen adsorption isotherms were measured at 77 K using a gas adsorption analyzer (Quantachrome Autosorb-1). Samples were preheated at 623 K for 12 h under a vacuum of  $10^{-4}$  Pa prior to the adsorption measurement. The BET method was applied to evaluate the total surface areas ( $S_{BET}$ ) (Brunauer et al., 1938). Mesopore size distributions (MPSDs) were determined from the nitrogen adsorption isotherms using the BJH method (Barret et al., 1951). Micropore structural parameters were determined on the basis of nitrogen adsorption isotherms using the Saito-Foley method with the cylindrical pore model (Saito and Foley, 1991; Saito and Foley, 1995).

### 2.2.2 FE-SEM

Morphologies of the representatives of alkaline-treated zeolites and the parent zeolites were observed under a field emission scanning electron microscope (JEOL, JSM-6330F). The samples were coated with osmium using an Osmium Coater Neoc-ST prior to the FE-SEM observation to avoid charge effect of the samples.

### 2.2.3 XRD

Powder X-ray diffraction (XRD) was carried out with a Miniflex X-ray automatic diffractometer (Rigaku Corporation.) using a monochromatized X-ray beam from nickel-filtered Cu K $\alpha$  ( $\lambda = 0.15406$  nm) radiation at room temperature and operated at 30.0 kV and 15.0 mA. The powder diffractograms of the samples were recorded over a range of  $2\theta$  values from  $5^\circ$  to  $60^\circ$ . The scanning rate was set at  $0.200^\circ/\text{min}$ .

### 2.2.4 FT-IR

The Fourier transform infrared (FT-IR) absorption spectra in the zeolite framework vibration region were obtained with FT/IR-410 spectrometer (JASCO Co.). Powder samples were dispersed in KBr pellets for FT-IR analysis. The spectrum was acquired in a wavenumber range between 400 and  $1500\text{ cm}^{-1}$  at  $2\text{ cm}^{-1}$  resolution.

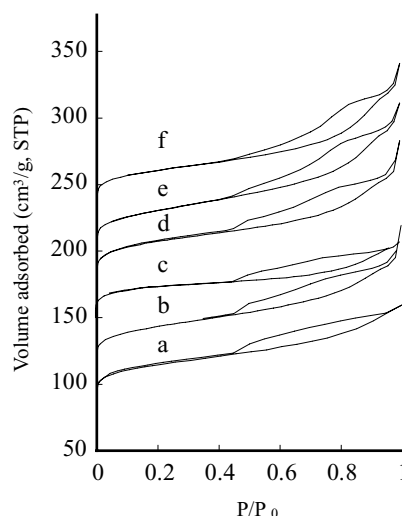


**Fig. 1** Adsorption/desorption isotherms of nitrogen at 77 K on the alkaline-treated ZSM-5 zeolites and the parent ZSM-5 zeolites: (a) ZSM-5[p], (b) ZSM-5[0.25 h], (c) ZSM-5[0.5 h], (d) ZSM-5[1.5 h], (e) ZSM-5[2 h], and (f) ZSM-5[4 h]. For clarity the isotherms have been shifted upwards with  $30\text{ cm}^3/\text{g}$  intervals between them.

## 3 Results and discussion

### 3.1 Pore structures

The nitrogen adsorption/desorption isotherms of the alkaline-treated ZSM-5 zeolites and the parent ZSM-5 zeolites are shown in Fig. 1. The nitrogen adsorption isotherm of parent zeolites was basically of IUPAC type I (Fig. 1a). Predominant adsorption ended below  $P/P_0 = 0.02$ , which is a characteristic of uniform microporous solids, while slight increase in higher relative pressure suggests nitrogen adsorption on external surfaces. The hysteresis loop of the nitrogen adsorption/desorption isotherms should result from the intercrystalline voids of the zeolite particles since each particle consists of many primary crystals. Recent investigation using mercury-intrusion porosity proved the existence of intercrystalline voids in the zeolite particle (Groen et al., 2006).

All alkaline-treated ZSM-5 zeolites have the same predominant adsorption ended below  $P/P_0 = 0.02$  as parent zeolites (Fig. 1b–f), indicating the preserved microporosity of the alkaline-treated zeolites. Compared with that of parent zeolites, all isotherms of alkaline treated zeolites show increase in uptake and change in the shapes of hysteresis loops extending from  $P/P_0 = 0.4$  to  $\sim 1$ , indicating the mesopores

**Table 1** Pore structural parameters and IR crystallinities of alkaline-treated ZSM-5 zeolites and parent zeolites

Sample	$S_{\text{BET}}$ [ $\text{m}^2\text{g}^{-1}$ ]	Microporosity		Mesoporosity		IR crystallinity [%]
		volume [ $\text{cm}^3\text{g}^{-1}$ ]	Size [nm]	volume [ $\text{cm}^3\text{g}^{-1}$ ]	Size [nm]	
ZSM-5[4 h]	329	0.16	0.55	0.12	2–25	85.5
ZSM-5[2 h]	342	0.16	0.55	0.12	2–25	85.8
ZSM-5[1.5 h]	328	0.16	0.55	0.14	10–20	84.0
ZSM-5[0.5 h]	336	0.16	0.55	0.06	2–35	85.3
ZSM-5[0.25]	339	0.16	0.55	0.10	2–35	83.2
ZSM-5[p]	336	0.16	0.55	0.05	2–30	84.0

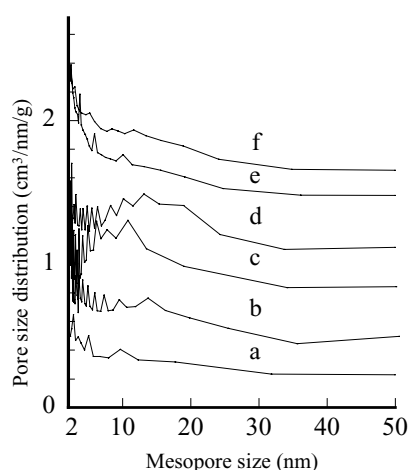


**Fig. 2** BJH mesopore size distributions obtained from nitrogen adsorption for the alkaline-treated ZSM-5 zeolites and the parent ZSM-5 zeolites: (a) ZSM-5[p], (b) ZSM-5[0.25 h], (c) ZSM-5[0.5 h], (d) ZSM-5[1.5 h], (e) ZSM-5[2 h], and (f) ZSM-5[4 h]. For clarity the curves have been shifted upwards with  $0.3 \text{ cm}^3/\text{nm/g}$  intervals between them.

that have been created upon alkaline treatments. The shapes of hysteresis loops tend to be of type H3, which generally obtained with adsorbents having slit-shaped pores or plate-like particulates (Gregg and Sing, 1982). Combined with the morphologies from the following FE-SEM images (Fig. 3), it is suggested that slit-shaped or ink-bottle-like mesopores grow mainly from the boundary portion of MFI zeolites to the bulk.

The mesopore size distributions (MPSDs) are shown in Fig. 2. As expected from the proposed mechanism of mesopore formation due to siliceous species selectively dissolving from the framework of zeolite (a lower amount of Al was also eluted) in previous studies (Ogura et al., 2000; Suzuki and Okuhara, 2001; Groen et al., 2002, 2004, 2005a, b, c), the mesopores with pore sizes of 2–35 nm are gradually developed before

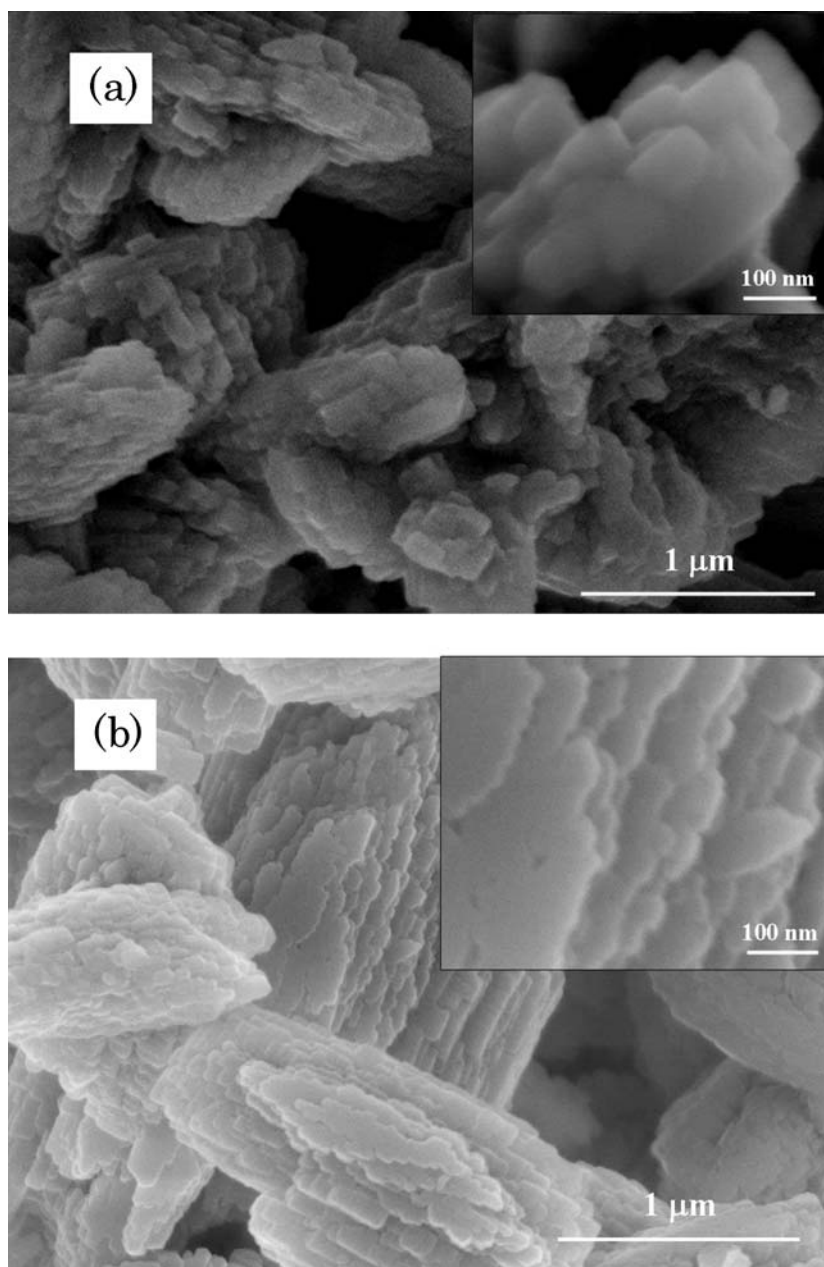
the 1.5 h treatment. Upon 1.5 h treatment, the MPSDs show a broad peak at 10–25 nm and a maximum of mesopore volume. Based on further prolonged alkaline treatments, MPSDs of ZSM-5[2 h] and ZSM-5[4 h] show mesopores mainly having pore size 2–10 nm with slight tail up to 25 nm. This infers that alkaline treatment longer than 1.5 h destroys most mesopores of 10–20 nm since the above-mentioned peak disappears, and the increased mesopores of 2–10 nm sizes shall be resulted from the piling up of small particles produced by the alkaline treatments.

Hence, alkaline treatment yields mesopores in ZSM-5 zeolite, and the pore developments and structures depend on the alkaline treatment periods. The parameters for the pore structure are listed in Table 1. The alkaline treatment period of  $\sim 1.5$  hours can be suggested for an optimal mesoporosity of greater mesopore volume and relatively uniform mesopore sizes.

### 3.2 Morphologies

The FE-SEM images for representatives of alkaline treated ZSM-5 zeolites and the parent ZSM-5 zeolites are shown in Fig. 3. Both low- and high-magnification SEM images of the parent ZSM-5 zeolites (Fig. 3a) show a quadrate surface morphology. Lattice fringes extend throughout the entire crystals, demonstrating the high crystallinity of the parent zeolites. The morphological changes of zeolite during the alkaline treatment appeared quite crucial. All FE-SEM images of the alkaline treated ZSM-5 zeolites seem polyhedron morphology. Some voids are observed on ZSM-5[1.5 h], and one can identify the voids of  $\sim 20$  nm width along the crystal edges from their high-magnification SEM image (Fig. 3b), which are comparable to the determined pore sizes from nitrogen adsorption. After prolonged

**Fig. 3** Field emission scanning electron micrographs of the alkaline-treated ZSM-5 zeolites and the parent ZSM-5 zeolites: (a) ZSM-5[p] and (b) ZSM-5[1.5 h]. The insets show both at high magnifications



treatment, voids disappeared and zeolites show outline sketch of smaller grains, supporting the previous analysis on the mesopore developments and structures. FE-SEM observations suggest that mild alkaline-treatment of zeolites develops mesopores in zeolites mainly along the edge of the crystals; while prolonged treatment brings to small zeolite grains and collapsed the formed mesoporous voids.

### 3.3 Crystalline structures

The crystallinities and unit framework structure in alkaline treated ZSM-5 zeolites were examined with X-ray diffractometry and Fourier transform infrared spectroscopy, respectively. The XRD patterns of alkaline treated zeolites and the parent zeolites are shown in Fig. 4. All XRD patterns of the samples before and after

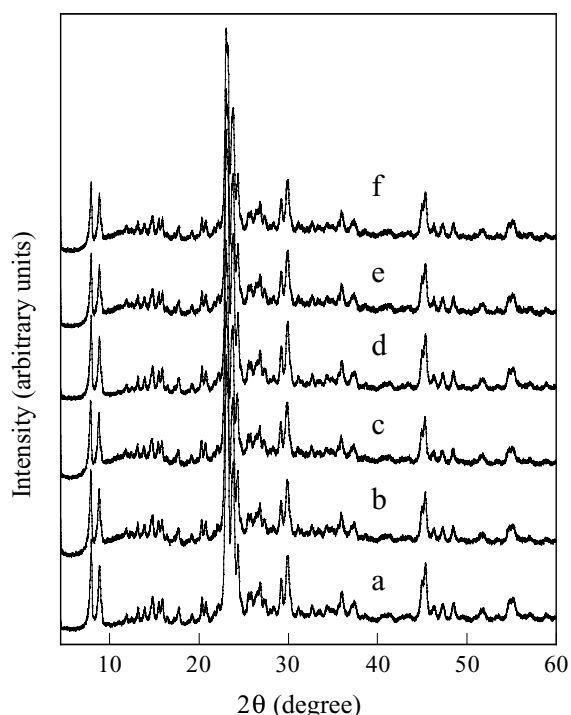


**Fig. 4** XRD powder patterns of alkaline-treated ZSM-5 zeolites and the parent ZSM-5 zeolites: (a) ZSM-5[p], (b) ZSM-5[0.25 h], (c) ZSM-5[0.5 h], (d) ZSM-5[1.5 h], (e) ZSM-5[2 h], and (f) ZSM-5[4 h]

alkaline treatment are consistent with those of well-ordered and pure phase ZSM-5 zeolites in literature (Argauer et al., 1972; Wu et al., 1979), suggesting the alkaline treatments lead to no change of the crystalline phases. No change in the XRD patterns with alkaline treatment indicates the alkaline treatment periods have no effect on their crystallinity and ordering.

The FT-IR spectra of alkaline treated zeolites and the parent zeolites are shown in Fig. 5. Compared with the parent zeolite reference, the FT-IR spectra of alkaline-treated ZSM-5 zeolites show the identical framework vibrations at  $550\text{ cm}^{-1}$ , which are characteristic double ring vibration in the MFI structured zeolites. Other absorption bands at  $1224\text{ cm}^{-1}$  (external asymmetric stretch),  $1150\text{--}1050\text{ cm}^{-1}$  (internal asymmetric stretch),  $795\text{ cm}^{-1}$  (external symmetric stretch), and  $455\text{ cm}^{-1}$  (T-O bend), which are typical for highly siliceous materials, were also identical with respect not only to the band positions but also to the peak intensity. The FT-IR examination further confirms the short-range order in alkaline treated ZSM-5 zeolites has remained virtually unchanged. For the determination

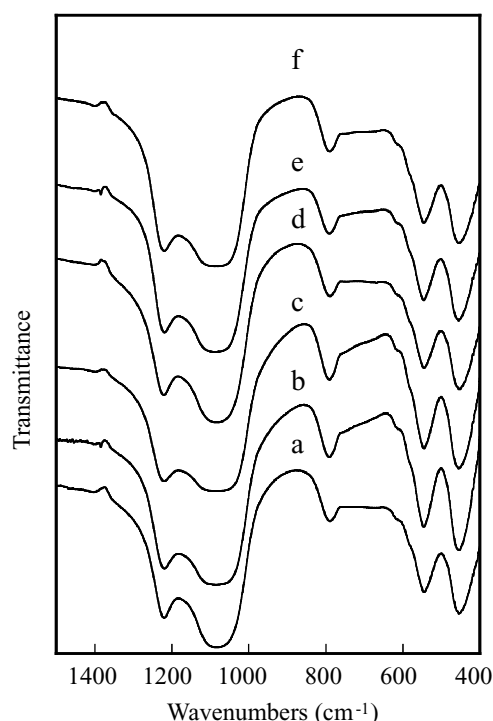


**Fig. 5** FT-IR spectra of the alkaline-treated ZSM-5 zeolites and the parent ZSM-5 zeolites: (a) ZSM-5[p], (b) ZSM-5[0.25 h], (c) ZSM-5[0.5 h], (d) ZSM-5[1.5 h], (e) ZSM-5[2 h], and (f) ZSM-5[4 h]

of the estimated purity of ZSM-5, the optical density ratio of the  $550$  and  $450\text{ cm}^{-1}$  bands in the IR spectrum was examined according to previous studies (Scholle et al., 1985; Jansen et al., 1984). Those of alkaline treated ZSM-5 zeolites and parent ZSM-5 are  $\sim 0.84$ , as presented in Table 1. Since the optical density ratio of all pure pentasil samples in the literature is 0.8 (Scholle et al., 1985; Jansen et al., 1984), the IR examination shows that all samples have a highly crystalline frame structure, meaning that the alkaline treatment did not change zeolite contents or crystallinities in the products.

#### 4 Conclusions

ZSM-5 zeolites with  $\text{SiO}_2/\text{Al}_2\text{O}_3$  molar ratio of 24 were treated in 0.05 M aqueous sodium hydroxide solution at 325 K in different periods, and it was found that the alkaline-treatment periods have influence on the developments and structures of mesopores. Alkaline treatment initially develops mesopores mainly proceeding from the boundary portion of MFI zeolites to the bulk,

while prolonged treatment destroys the mesopores. Alkaline treated zeolites do not possess a uniform pore size distribution, however, an optimal treatment condition for a mesoporosity of greater mesopore volume and relatively uniform mesopore sizes can be determined. The crystallinities and short-range order of zeolites are preserved on the alkaline treatment. As the present mild alkaline-treatment can produce mesoporous zeolites on a relatively larger scale, the effect of mesopores on catalytic reactions can be more clearly clarified.

**Acknowledgment** The authors thank Dr. M. Nakano and Mr. S. Yosida, Tosoh Corporation for kind supply of zeolite samples. Y. Tao acknowledges a postdoctoral fellowship for foreign researchers from Japan Society for the Promotion of Science (JSPS).

## References

- Argauer, R.J. and G.R. Landolt, "Crystalline Zeolite ZSM-5 and Method of Preparing the Same," U.S. Patent 3702886 (1972).
- Barret, P., L.G. Joyner, and P.P. Halenda, "The Determination of Pore Volume and Area Distributions in Porous Substances. I. Computations from Nitrogen Isotherms," *J. Am. Chem. Soc.*, **73**, 373–380 (1951).
- Breck D.W., *Zeolite Molecular Sieves*, pp. 64–67, Robert E. Krieger Publishing Company, Malabar, FL, 1974.
- Brunauer S., P.H. Emmett, and E. Teller, "Adsorption of Gases in Multimolecular Layers," *J. Am. Chem. Soc.*, **60**, 309–319 (1938).
- Carlidge, S., H.-U. Nissen, and R. Wessicken, "Ternary Mesoporous Structure of Ultraporous Zeolite CSZ-1," *Zeolites*, **9**, 346–349 (1989).
- Chen N.Y. and T.F. Degnan, "Industrial Catalytic Applications of Zeolites," *Chem. Eng. Prog.*, **84**, 32–41 (1988).
- Choi-Feng, C., J.B. Hall, B.J. Huggins, and R.A. Begerlein, "Electron Microscope Investigation of Mesopore Formation and Aluminum Migration in USY Catalysts," *J. Catal.*, **140**, 395–405 (1993).
- Christensen, C.H., I. Schmidt, A. Carlsson, K. Johannsen, and K. Herbst, "Crystals in Crystals-Nanocrystals within Mesoporous Zeolite Single Crystals," *J. Am. Chem. Soc.*, **127**, 8098–8102 (2005).
- Cizmek, B., B. Suboti, R. Aiello, F. Crea, A. Nastro, and C. Tuoto, "Dissolution of High-silica Zeolites in Alkaline Solutions I. Dissolution of Silicalite-1 and ZSM-5 with Different Aluminum Content," *Microporous Materials*, **4**, 159–168 (1995).
- Cizmek, B., B. Suboti, I. Smit, A. Tonejc, R. Aiello, F. Crea, and A. Nastro, "Dissolution of High-silica Zeolites in Alkaline Solutions II. Dissolution of 'Activated' Silicalite-1 and ZSM-5 with Different Aluminum Content," *Microporous Mater.*, **8**, 159–169 (1997).
- Corma, A., "From Microporous to Mesoporous Molecular Sieve Materials and Their Use in Catalysis," *Chem. Rev.*, **97**, 2373–2420 (1997).
- Corma, A., M.J. Diaz-Cabanas, J. Martinez-Triguero, F. Rey, and J. Rius, "A Large-cavity Zeolite with Wide Pore Windows and Potential as an Oil Refining Catalyst," *Nature*, **418**, 514–517 (2002).
- Corma, A., "State of the Art and Future Challenges of Zeolites as Catalysts," *J. Catal.*, **216**, 298–312 (2003).
- Davis, M.E., "Ordered Porous Materials for Emerging Applications," *Nature*, **417**, 813–821 (2002).
- Ghose S. and B. Mattiasson, "Protein Adsorption to Hydrophobic Zeolite Y: Salt effects and Application to Protein Fractionation," *Biotechnol. Appl. Biochem.*, **18**, 311–320 (1993).
- Gregg, S.J. and K.S.W. Sing, *Adsorption, Surface Area and Porosity*, pp 111–194, 2nd edition, Academic Press, London, 1982.
- Groen, J.C., J.A. Moulijn, and J. Pérez-Ramírez, "Decoupling Mesoporosity Formation and Acidity Modification in ZSM-5 Zeolites by Sequential Desilication–dealumination," *Microporous Mesoporous Mater.*, **87**, 153–161 (2005a).
- Groen, J.C., J.C. Jansen, J.A. Moulijn, and J. Pérez-Ramírez, "Optimal Aluminum-Assisted Mesoporosity Development in MFI Zeolites by Desilication," *J. Phys. Chem. B*, **108**, 13062–13065 (2004).
- Groen, J.C., J. Pérez-Ramírez, and L.A.A. Pfeffer, "Formation of Uniform Mesopores in ZSM-5 Zeolite upon Alkaline Post-treatment," *Chem. Lett.*, 94–94 (2002).
- Groen, J.C., L.A.A. Pfeffer, and J. Pérez-Ramírez, "Pore Size Determination in Modified Micro- and Mesoporous Materials. Pitfalls and Limitations in Gas Adsorption Data Analysis," *Microporous Mesoporous Mater.*, **60**, 1–17 (2003).
- Groen, J.C., L.A.A. Pfeffer, J.A. Moulijn, and J. Pérez-Ramírez, "Mechanism of Hierarchical Porosity Development in MFI Zeolites by Desilication: The Role of Aluminium as a Pore-Directing Agent," *Chem. Eur. J.*, **11**, 4983–4994 (2005b).
- Groen, J.C., S. Brouwer, L.A.A. Pfeffer, and J. Pérez-Ramírez, "Application of Mercury Intrusion Porosimetry for Characterization of Combined Micro- and Mesoporous Zeolites," *Part. Part. Syst. Charact.*, **23**, 101–106 (2006).
- Groen, J.C., T. Bach, U. Ziese, A.M. Paulaime-van Donk, K.P. de Jong, J.A. Moulijn, and J. Pérez-Ramírez, "Creation of Hollow Zeolite Architectures by Controlled Desilication of Al-Zoned ZSM-5 Crystals," *J. Am. Chem. Soc.*, **127**, 10792–10793 (2005c).
- Hartman, M., "Hierarchical Zeolites: A Proven Strategy to Combine Shape Selectivity with Efficient Mass Transport," *Angew. Chem. Int. Ed.*, **43**, 5880–5882 (2004).
- Herrmann, C., J. Haas, and F. Fetting, "Effect of the Crystal Size on the Activity of ZSM-5 Catalysts in Various Reactions," *Appl. Catal.*, **35**, 299–310 (1987).
- Jacobsen, C.J.H., C. Madsen, J. Houzvicka, I. Schmidt, and A. Carlsson, "Mesoporous Zeolite Single Crystals," *J. Am. Chem. Soc.*, **122**, 7116–7117 (2000).
- Jansen, J.C., F.J. van der Gaag, and H. van Bekkum, "Identification of ZSM-type and Other 5-ring Containing Zeolites by i.r. Spectroscopy," *Zeolites*, 369–372 (1984).
- Janssen, A.H., I. Schmidt, C.J.H. Jacobsen, A.J. Koster, and K.P. de Jong, "Exploratory Study of Mesopore Templating with Carbon During Zeolite Synthesis," *Microporous Mesoporous Mater.*, **65**, 59–75 (2003).
- Kärger J. and D.M. Ruthven, *Diffusion in Zeolites and Other Microporous Materials*, pp. 375–426, Wiley, New York, 1992.

- Lynch, J., F. Raatz, and P. Dufresne, "Characterization of the Textural Properties of Dealuminated HY Forms," *Zeolites*, **7**, 333–340 (1987).
- Ogura, M., S. Shinomiya, J. Tateno, Y. Nara, E. Kikuchi, and M. Matsukata, "Formation of Uniform Mesopores in ZSM-5 Zeolite through Treatment in Alkaline Solution," *Chem. Lett.*, 882–883 (2000).
- Ogura, M., S. Shinomiya, J. Tateno, Y. Nara, M. Nomura, E. Kikuchi, and M. Matsukata, "Alkali-treatment Technique – New Method for Modification of Structural and Acid-catalytic Properties of ZSM-5 Zeolites," *Appl. Catal. A*, **219**, 33–43 (2001).
- Patzelová, V. and N.I. Jaeger, "Texture of Deep Bed Treated Y Zeolites," *Zeolites*, **7**, 240–242 (1987).
- Perez-Ramirez J., F. Kapteijn, J.C. Groen, A. Domenech, G. Mul, and J.A. Moulijn, "Steam-activated FeMFI Zeolites. Evolution of Iron Species and Activity in Direct N<sub>2</sub>O Decomposition," *J. Catal.*, **214**, 33–45 (2003).
- Pires J., A. Carvalho, and M.B. de Carvahlo, "Adsorption of Volatile Organic Compounds in Y Zeolites and Pillared Clays," *Micropor. Mesopor. Mater.*, **43**, 277–287 (2001).
- Richter M., H. Berndt, R. Eckelt, M. Schneider, and R. Fricke, "Zeolite-mediated Removal of NO<sub>x</sub> by NH<sub>3</sub> from Exhaust Streams at Low Temperatures," *Catalysis Today*, **54**, 531–545 (1999).
- Saito, A. and H.C. Foley, "Argon Porosimetry of Selected Molecular Sieves: Experiments and Examination of the Adapted Horvath-Kawazoe Model," *Microporous Mater.*, **3**, 531–542 (1995).
- Saito, A. and H.C. Foley, "Curvature and Parametric Sensitivity in Models for Adsorption in Micropores," *AIChE J.*, **37**, 429–436 (1991).
- Sakthivel, A., S. Huang, W. Chen, Z. Lan, K. Chen, T. Kim, R. Ryoo, A.S.T. Chiang, and S. Liu, "Replication of Mesoporous Aluminosilicate Molecular Sieves (RMMs) with Zeolite Framework from Mesoporous Carbons (CMKs)," *Chem. Mater.*, **16**, 3168–3175 (2004).
- Schmidt, I., A. Boisen, E. Gustavsson, K. Stahl, S. Pehrson, S. Dahl, A. Carlsson, and C.J.H. Jacobsen, "Carbon Nanotube Templated Growth of Mesoporous Zeolite Single Crystals," *Chem. Mater.*, **13**, 4416–4418 (2001).
- Scholle, K.F.M.G.J., W.S. Veeman, P. Frenken, and G.P.M. van der Velden, "Characterization of Intermediate TPA-ZSM-5 Type Structures During Crystallization," *Appl. Catal.*, **17**, 233–259 (1985).
- Smith, J.V., "Topochemistry of Zeolites and Related Materials. 1. Topology and Geometry," *Chem. Rev.*, **88**, 149–182 (1988).
- Suzuki, T. and T. Okuhara, "Change in Pore Structure of MFI Zeolite by Treatment with NaOH Aqueous Solution," *Micropor. Mesopor. Mater.*, **43**, 83–89 (2001).
- Tao, Y., H. Kanoh, and K. Kaneko, "ZSM-5 Monolith of Uniform Mesoporous Channels," *J. Am. Chem. Soc.*, **125**, 6044–6045 (2003).
- Tao, Y., H. Kanoh, J.C. Groen, and K. Kaneko, "Characterization of Alkaline Post-treated ZSM-5 Zeolites by Low Temperature Nitrogen adsorption," *Stud. Surf. Sci. Catal.*, in press.
- Tao, Y.H., Kanoh, L. Abrams, and K. Kaneko, "Mesopore-Modified Zeolites: Preparation, Characterization, and Applications," *Chem. Rev.*, **106**, 896–910 (2006).
- van Donk, S., A. Broersma, O.L.J. Gijzeman, J.A. van Bokhoven, J.H. Bitter, and K.P. de Jong, "Combined Diffusion, Adsorption, and Reaction Studies of *n*-Hexane Hydroisomerization over Pt/H–Mordenite in an Oscillating Microbalance," *J. Catal.*, **204**, 272–280 (2001).
- van Donk, S., A.H. Janssen, J.H. Bitter, and K.P. de Jong, "Generation, Characterization, and Impact of Mesopores in Zeolite Catalysts," *Catal. Rev.*, **45**, 297–319 (2003).
- Wu, E.L., S.L. Lawton, D.H. Olson, A.C., Jr. Rohrman, and G.T. Kokotailo, "ZSM-5-Type Materials. Factors Affecting Crystal Symmetry," *J. Phys. Chem.*, **83**, 2777–2781 (1979).
- Yang, Z., Y. Xia, and R. Mokaya, "Zeolite ZSM-5 with Unique Supermicropores Synthesized Using Mesoporous Carbon as a Template," *Adv. Mater.*, **16**, 727–732 (2004).